LIMNOLOGY and OCEANOGRAPHY

ASLO

Limnol. Oceanogr. 65, 2020, 2787–2799

doi: 10.1002/lno.11552

Resolving marine dissolved organic phosphorus (DOP) composition in a coastal estuary

Douglas W. Bell,[1*] **Perry J. Pellechia**,[2] **Ellery D. Ingall**,[3] **Claudia R. Benitez-Nelson**[1]

[1]School of the Earth, Ocean, and Environment, University of South Carolina, Columbia, South Carolina
[2]Department of Chemistry and Biochemistry, University of South Carolina, Columbia, South Carolina
[3]Department of Earth & Atmospheric Sciences, Georgia Institute of Technology, Atlanta, Georgia

Abstract

A mechanistic understanding of dissolved organic phosphorus (DOP) utilization, and its role in the marine P cycle, requires knowledge of DOP molecular composition. In this study, a recently developed approach coupling electrodialysis and reverse osmosis with solution ^{31}P-NMR analysis was used to examine DOP composition within a tidally dominated salt-marsh estuary (North Inlet, South Carolina) over seasonal and tidal time frames. The isolation technique allowed for near complete recovery of the DOP pool (90% ± 13%; n = 12) with six broad compound classes quantified: phosphonates, phosphomonoesters, phosphodiesters, pyrophosphate, di- and tri-phosphate nucleotides (nucleoP$_\alpha$), and polyphosphate. Our results indicate that phosphomonoesters (ca. 61%) and phosphodiesters (ca. 31%) comprise the majority of the DOP pool, with relatively small contributions from pyrophosphates (ca. 4%), phosphonates (ca. 2%), nucleoP$_\alpha$ (ca. 1%), and polyphosphates (ca. 1%). The study found no significant differences in DOP composition or concentration between tidal stages, despite significant tidal changes in dissolved organic nitrogen (DON):DOP stoichiometry. Significant seasonal variation was observed, with higher concentrations of phosphonates, nucleoP$_\alpha$, and monophosphates and lower phosphomonoester concentrations in Fall relative to all other seasons. We hypothesize that these seasonal variations reflect the balance between specific compound class seasonal production, lability, and local P demands associated with marine vs. terrestrial sources. Our results indicate that DOP composition exists at a dynamic equilibrium that is strongly conserved across diverse marine environments.

The supply and composition of phosphorus (P) directly impacts marine microorganism production and community composition (Karl 2014). In turn, these communities shape the magnitude and rate of numerous marine biogeochemical cycles, ultimately affecting global climate and marine food webs (Arrigo 2005). However, due to limitations in analytical discrimination and differential biological capacity for dissolved organic P (DOP) uptake, the biologically available supply (i.e., bioavailability) of P to marine organisms has been notoriously difficult to define (Karl and Björkman 2015). This uncertainty prevents a mechanistic understanding of P utilization and turnover on biological timescales, which affects the accuracy of biogeochemical models of global carbon cycling (Letscher and Moore 2015) and the scientific underpinning for managing the consequences of eutrophication (Howarth et al. 2011).

Defining P bioavailability across marine taxa is challenging due to the diverse and species-specific physiological strategies utilized in response to P concentration and composition (Ruttenberg and Dyhrman 2005). To accommodate their relative P demand, phytoplankton and heterotrophic bacteria can adjust their P acquisition through three predominant mechanisms: differential expression of inorganic phosphate (P_i) transport systems to adjust external P_i uptake kinetics (Lin et al. 2016), internal control of P requirements (Van Mooy et al. 2009), and the utilization of DOP through compound-specific hydrolytic enzymes (Cembella et al. 1982). In demonstration of the later strategy, Yamaguchi et al. (2005) observed *Chaetoceros ceratosporus* to be the only phytoplankton species (out of five evaluated) that was able to grow with DOP as the sole P source, which was reinforced by high levels of corresponding hydrolytic enzyme activity. The ability to utilize DOP dramatically increases the potential supply of P and an increasing number of studies continue to demonstrate the potential demand for DOP, including a specificity in the type of compound classes utilized (Luo et al. 2009; Martinez et al. 2010). As a result, DOP utilization is a key biological trait used to explain the complex trends of P stress, limitation, and

*Correspondence: doug.bell@noaa.gov

Additional Supporting Information may be found in the online version of this article.

co-limitation in the marine environment (Moore et al. 2013), preferential remineralization of dissolved organic matter (DOM; Clark et al. 1998, Hopkinson et al. 2002), and rates of DOP turnover, which range from less than a day to months in the marine environment (Lønborg and Álvarez-Salgado 2012; Karl 2014). Given the selective utilization of certain compound classes by microorganisms, a primary technical barrier to defining P bioavailability has therefore been identifying the composition of the DOP pool.

Despite technical advances in the identification and quantification of P-containing compound and biomolecule classes (Diaz et al. 2008; Van Mooy et al. 2009; Kujawinski et al. 2017), there remains a significant lack of knowledge regarding the composition of marine DOP at the molecular level scale. At present, a complete picture of DOP composition is hindered by overlapping compound reactivities inherent to each method of analysis (Karl 2014). ^{31}P-NMR spectroscopy, which does not rely on reactivity, has been demonstrated to be an effective tool for identification of different P compound classes in environmental biogeochemistry studies (Cade-Menun 2005; Simpson et al. 2012). A major limitation of DOP-specific ^{31}P-NMR spectroscopy, however, is the sample mass required for a quantitative signal. The collection of DOP from seawater, and to a broader extent, DOM, requires concentration and purification from an ionized salt matrix (Green et al. 2014). Kolowith et al. (2001) used ultrafiltration-isolation (molecular weight >1000 Da) to determine that phosphoesters and phosphonates are the two dominant classes of the high molecular weight (HMW) fraction of marine DOP (i.e., ultrafiltered or UDOP). Yet the majority fraction of the DOP pool remained unexplored due to the inherent molecular size bias of ultrafiltration (the HMW fraction comprises only ~ 20–40% of DOM). Since then, DOM isolation has steadily improved due to advances in solid phase extraction resin techniques and the development of coupled electrodialysis and reverse osmosis techniques (ED/RO) (Chambers et al. 2016). The ED/RO isolation procedure has been shown to recover relatively large amounts of dissolved organic carbon (DOC) relative to other techniques (ca. 68%; Chambers et al. 2016, and sources therein), but equally important is the technique's conservation of sample compositional integrity (Green et al. 2014). Recently, Young and Ingall (2010) applied ED/RO to isolate and concentrate DOP for ^{31}P-NMR characterization, updating current estimates of bulk DOP composition by including the minor, but consistent presence of the phosphoanhydride class. However, this assessment employed solid-state ^{31}P-NMR spectrscopy, which has limited compound class resolution due to broad overlapping resonances that are caused by the presence of paramagnetic ions (e.g., Fe) and large chemical shift anisotropy (Cade Menun 2005).

Solution-state ^{31}P-NMR achieves greater spectral resolution while also requiring less sample material, presenting a relatively unexplored opportunity for assessing marine DOP (Cade-Menun 2015). Solution ^{31}P-NMR accomplishes this by use of an extraction step and solubilization during analysis. Extraction reduces P complexation with paramagnetic ions, while solubilization allows for non-static molecular behavior, which enhances signal resolution. However, this technique does come at the risk of compound hydrolysis and preferential extraction (Cade-Menun 2005). Recently, we tested a coupled ED/RO isolation and solution-state ^{31}P-NMR approach to determine its efficacy for DOP isolation and compositional analysis (Bell et al. 2017). Our work demonstrated that ED/RO recovers a significant majority ($83.8\% \pm 10.7\%$) of the DOP pool with minimal isolation biases, while solution ^{31}P-NMR allowed for the semi-quantification of several newly resolved molecular subclasses of DOP (Bell et al. 2017).

Here, we present an updated estimate on the molecular composition of DOP using ED/RO and solution ^{31}P-NMR. To date, similar studies that have utilized ^{31}P-NMR techniques have reported a remarkable level of consistency across a broad range of marine environments, including intra-water column similarities. In this study, samples were collected at high and low tide, twice per season, from a single collection site within a tidally dominated salt-marsh estuary. The salt-marsh estuary serves multiple purposes for this study. First, the study occurred within a National Estuarine Research Reserve System (NERRS) site, which provided accompanying water quality monitoring data and a multi-decade history of biogeochemical research. Second, tidal sampling provided an opportunity to assess the potential transformation of DOP across the land–ocean continuum, specifically, the source variability between the *Spartina*-dominated salt marsh and an adjacent freshwater swamp, with a near-shore coastal ocean. Finally, given the accompanying monitoring data and site accessibility, this study was able to evaluate the seasonal transition of light- and temperature-sensitive processes (i.e., primary production, microbial respiration), which ultimately shape the cycling of DOP.

Methods

Sample collection

Water was collected at Oyster Landing (OL), a monitoring site within a bar-built, tidally dominated estuary (North Inlet, Georgetown County, South Carolina; Fig. 1). The tidal-creek system sits within the greater North Inlet-Winyah Bay Estuarine Research Reserve, which is part of the NERRS. North Inlet is minimally impacted by anthropogenic forcing and receives relatively low inputs of freshwater, reflected by daily salinities that range between 30 and 34 (Gardner et al. 2006). Sampling was conducted twice per season from August 2014 through August 2015 at slack high and low tide of the same tidal cycle (n = 15). Samples were collected at 0.5 m below the surface (OL depth = 2 m; mean semi-diurnal tidal range = 1.5 m; Gardner et al. 2006) in acid-rinsed, high-density polyethylene containers. Samples for DOP ^{31}P-NMR analysis were

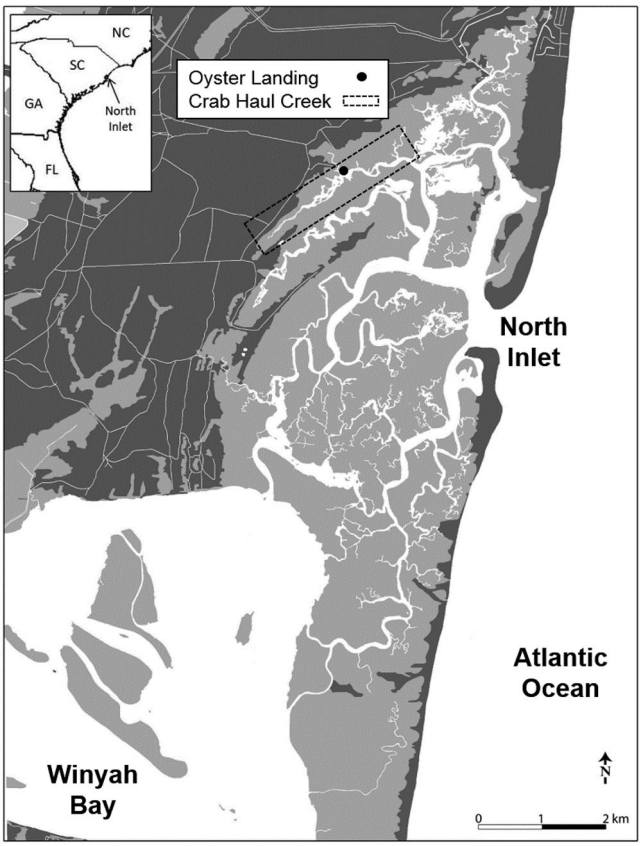

Fig. 1. North Inlet – Winyah Bay National Estuarine Research Reserve (NERR) located near Georgetown, South Carolina. Oyster Landing (NERR monitoring site) is starred within Crab Haul Creek.

immediately filtered through an acid-rinsed 10.85 inch 0.2 μm cartridge filter (Flotrex ™ FPN921EGV; GE Water Processes and Technologies) and stored in the dark at 4°C until ED/RO processing (1–4 d later). Samples for suspended particulates were collected onto acid-washed, pre-combusted GF/F filters (0.7-μm nominal pore size, Whatman). Aliquots from the filtrate were collected for dissolved nutrient analyses. Analytical methods for water chemistry samples are further described within the Supplemental Material.

Isolation

A detailed description of the ED/RO isolation process, including instrument operation and an assessment of P recovery, mass balance, and isolation biases is found in Bell et al. (2017). Briefly, prior to isolation, the ED/RO system undergoes an acidic and alkaline cleaning treatment. The system was first preconditioned with 2 L of sample. The remaining 12 L of sample was then added to the ED/RO sample reservoir and diluted with 3 L of 18.2 Ω deionized water (DIW) to reduce the initial electric potential of the ED process. Sample isolation began exclusively with ED until the sample reached a threshold conductivity of 5 mS, at which the coupled ED/RO process was performed until the sample volume was reduced to ca. 800 mL (minimal volume for circulation). Electrodialysis was then repeated until sample conductivity was reduced to ca. 1 mS. The isolated sample was then drained from all ED/RO reservoirs, the ED/RO instrument soaked and rinsed with a known volume of DIW (~ 800 mL), and the solution added to the final isolated sample. This process was slightly modified from the first set of samples collected during the fall (OL1–OL2). Instead of single batch processing, sequential additions of sample were added once the sample was reduced to the minimum circulation volume (totaling 6–8, 12 L batches). Sequential batch processing, however, was a considerably longer process, taking nearly 30 h to complete the ED/RO isolation process per sample. Single batch processing took roughly 8 h, a reasonable amount of time for repetitive sample processing, which was a consideration to facilitate adoption of ED/RO isolation. In addition, sequential batch processing resulted in greater recovery uncertainties due to analytical error propagation of the low P concentrations in each initial batch-sample.

Recovery estimates of the liquid isolate were determined by colorimetric detection (Beckman Coulter DU640 spectrophotometer) of soluble reactive P (SRP) and total dissolved P (TDP) using the Koroleff (1983) method and a modified Monaghan and Ruttenberg (1999) technique. DOP was determined as the difference between TDP and SRP (i.e., DOP = TDP − SRP). Liquid sample isolates were then lyophilized in 35 mL aliquots and dried material was measured for total particulate P and particulate inorganic P (TPP and PIP, respectively) to assess the concentration and P speciation prior to ^{31}P-NMR dissolution. Total particulate P and PIP concentrations were determined using a modified Aspila et al. (1976) method. Particulate organic P (POP) was operationally defined as the difference between total and inorganic fractions (POP = TPP − PIP).

^{31}P-NMR analysis

Sample preparation for solution ^{31}P-NMR is described in detail by Bell et al. (2017) with the following amendments. Lyophilized material (ca. 0.36 g) was dissolved in 275 μL of deuterium oxide (D_2O, Sigma-Aldrich), 275 μL NaOH-EDTA (0.25 M and 0.05 M, respectively), and 275 μL of 10 M NaOH (sample pH > 12) in a 15 mL polypropylene centrifuge tube (VWR), following the dissolution procedure described in Cade-Menun (2015). Separate experimental testing (*see* Supplemental Material) also examined potential changes in P speciation under simulated ^{31}P-NMR experimental conditions and the effect of different material loads on sample dissolution. Dissolved samples were vortexed for ~ 2 min, then centrifuged for 5 min at 1500 rpm (r = 22.5 cm). Supernatant was aspirated into a 1.5 mL polypropylene microcentrifuge tube (USA Scientific) and the residual pellet was diluted with DIW, neutralized, and frozen for TDP and SRP analysis. Subsamples (50 μL) of the supernatant were also collected, diluted, and neutralized for selected samples, and then frozen for TDP and

Table 1. Isolation recovery estimates and integrity proxies for each analytical phase (organic phosphorus composition; %OP). "Recovery" data includes the percent of dissolved organic P (DOP) recovered using electrodialysis-reverse osmosis (ED/RO) isolation, the total mass of P, and the concentration of lyophilized isolate. The integrity of the isolate was tracked in the final ED/RO isolate phase (Iso), after lyophilization (Lyo), upon immediate re-dissolution prior to ^{31}P-NMR analysis (Diss), and from the ^{31}P-NMR spectra (NMR). Individual error is included in parentheses, while the average error associated with the Iso, Lyo, Diss, and NMR phases was approximately 5%, 4%, 6%, and 3%.

			Recovery			Iso	Lyo	Diss	NMR
ID	Date	Tide	%DOP	μmol P	μmol P g^{-1}	%OP	%OP	%OP	%OP
OL1	30 Oct 2014	High	*	7.5 (0.5)	10.4 (0.2)	93 (11)	95 (2)	96 (1)	95 (3)
		Low	*	9.5 (0.3)	8.5 (0.2)	91 (5)	94 (3)		96 (3)
OL2	19 Nov 2014	High	*	6.5 (0.1)	16.1 (0.2)	95 (2)	94 (2)		92 (3)
OL3	07 Feb 2015	High	86 (9)†	2.8 (0.2)	1.4 (0.0)	96 (12)	93 (2)	95 (10)	92 (3)
		Low	106 (10)†	4.9 (0.3)	1.8 (0.0)	93 (8)	88 (1)	93 (17)	83 (3)
OL4	27 Feb 2015	High	110 (5)†	2.0 (0.0)	3.7 (0.1)	80 (3)	89 (4)		87 (3)
		Low	73 (4)	1.0 (0.0)	3.2 (0.1)	82 (4)	92 (6)	84 (7)	80 (3)
OL5	28 Apr 2015	High	99 (11)†	3.4 (0.1)	2.5 (0.0)	91 (3)	87 (4)	89 (1)	86 (3)
		Low	100 (6)	7.8 (0.3)	3.0 (0.2)	88 (6)	84 (8)	82 (2)	84 (3)
OL6	18 May 2015	High	93 (8)†	2.5 (0.1)	2.1 (0.1)	91 (8)	84 (8)		86 (3)
		Low	81 (5)	6.9 (0.2)	3.2 (0.0)	84 (4)	85 (2)	90 (1)	89 (3)
OL7	17 Jul 2015	High	76 (10)	2.8 (0.0)	2.0 (0.1)	87 (1)	82 (6)	88 (7)	79 (3)
		Low	97 (6)	9.3 (0.2)	3.5 (0.1)	86 (3)	86 (5)		89 (3)
OL8	06 Aug 2015	High	78 (9)	3.1 (0.1)	2.5 (0.0)	91 (6)	89 (2)	87 (4)	82 (3)
		Low	81 (8)	7.3 (0.1)	2.5 (0.1)	80 (3)	91 (6)	94 (10)	92 (3)

*Isolation procedure attempted sequential batch processing that produced large uncertainties with recovery estimates (80–160%).
†Calculations include near or below detection limit SRP and/or suspected incomplete initial circulation.

Table 2. Composition of dissolved organic phosphorus (DOP) from the North Inlet estuary. The P mass analyzed by solution ^{31}P-NMR is given in the "Sample" column with the estimated percent that dissolved into the matrix (% diss). Quantifiable components were: phosphonates (Pnate), monoesters (monoP), diesters (diP), pyrophosphate (pyroP), ester nucleotide-P (nucleo-P_α), and long-chain polyphosphate (polyP). The spectra shift(s) is below each component's header (in ppm). The raw error of component estimates (i.e., instrumentation and post-processing) is approximately ± 5%.

		Sample		Pnate	monoP	diP	pyroP	nucleoP_α	polyP
				27 to 23	5 to 2	2 to −4	−4.1	−9 to −12	−15 to −25
ID	Tide	μmol P	% diss	%	%	%	%	%	%
OL1	High	2.42 (0.06)	79 (2)	10	51	36	3	0	0
	Low	1.95 (0.05)	69 (2)	11	41	38	5	6	0
OL2	High	1.53 (0.04)	62 (2)	11	49	32	3	5	0
OL3	High	0.49 (0.01)	57 (19)	0	67	30	3	0	0
	Low	0.42 (0.01)	67 (1)	0	63	26	5	0	7
OL4	High	0.31 (0.01)	66 (3)	0	68	25	7	0	0
	Low	0.84 (0.05)	72 (5)	0	60	30	4	0	5
OL5	High	0.88 (0.01)	46 (31)	0	68	25	6	0	0
	Low	1.07 (0.05)	55 (13)	0	63	33	4	0	0
OL6	High	0.55 (0.04)	72 (6)	0	64	33	2	0	0
	Low	0.73 (0.01)	63 (1)	0	70	27	3	0	0
OL7	High	0.38 (0.02)	55 (4)	0	59	41	0	0	0
	Low	0.66 (0.04)	52 (4)	0	58	27	6	0	2
OL8	High	1.11 (0.04)	64 (5)	0	69	23	8	0	0
	Low	0.60 (0.04)	55 (5)	0	64	32	3	0	0

SRP analysis. Samples were chilled (4°C) for a maximum of 2 h prior to the ^{31}P-NMR experiment. The integrity of the isolate was thus tracked through P measurements in the final ED/RO isolate phase (Iso), after lyophilization (Lyo), upon immediate re-dissolution prior to ^{31}P-NMR analysis (Diss) and using the ^{31}P-NMR spectra (NMR).

Solution ^{31}P-NMR experiments were performed as described by Bell et al. (2017) on a Bruker Avance III-HD 400 MHz using a 5-mm broadband Prodigy cryoprobe. The T_1 relaxation times (0.9–2.9 s) were determined for a series of DOP compound standards. Samples with unknown composition were run with a 10 s relaxation delay (i.e., slightly greater than 3× maximum T_1). Spectra were collected with inverse gated (i.e., nuclear Overhauser effect suppressed) broadband decoupling and shifts are reported in parts per million (ppm) compared to an external standard (85% phosphoric acid). Bruker Topsin 3.5 was used for post-processing results. Deconvolution was completed using Mestrelab MNova v.10. Experiments were typically run for ~ 7 to 9 h, with two samples run for ~ 13 and ~ 20 h. Temperatures were kept at 15°C throughout the experiments.

Compound classes were defined over the following spectral shifts/peaks (similar to Cade-Menun 2005): phosphonate (27–23 ppm; Pnate), orthophosphate (ca. 5.5 ppm; orthoP), orthophosphatemonoester-P (ca. 5.5–2 ppm; monoP), orthophosphatediester-P (2 to approximately −4 ppm; diP), pyrophosphate (ca. −4.1 ppm; pyroP), nucleotide ester-linked P (α group on di- or tri-phosphate chain; −9 to −12 ppm; nucleoP$_\alpha$); long-chain polyphosphate (−15 to −25 ppm; polyP). Previous compound-specific testing (Bell et al. 2017) provided a reference shift library under similar analytical (i.e., D_2O and NaOH) and environmental (i.e., North Inlet DOM) matrixes, while Cade-Menun (2015) provides an even larger reference shift library in a matching analytical matrix. The orthophosphate shift observed in each individual spectrum provides an independent reference point between both compound libraries and individual samples.

To quantify each compound class, several post-processing techniques (backward linear prediction, digital filtering, baseline correction) were applied to reduce background noise and establish a corrected baseline. Peak and peak ranges were integrated over the defined compound classes and defined by natural inflection points when appropriate. This was often done with diP and pyroP where peaks overlapped. Spectrum peaks or peak ranges that had a signal-to-noise (S/N) ratio < 2 were excluded from integration. The

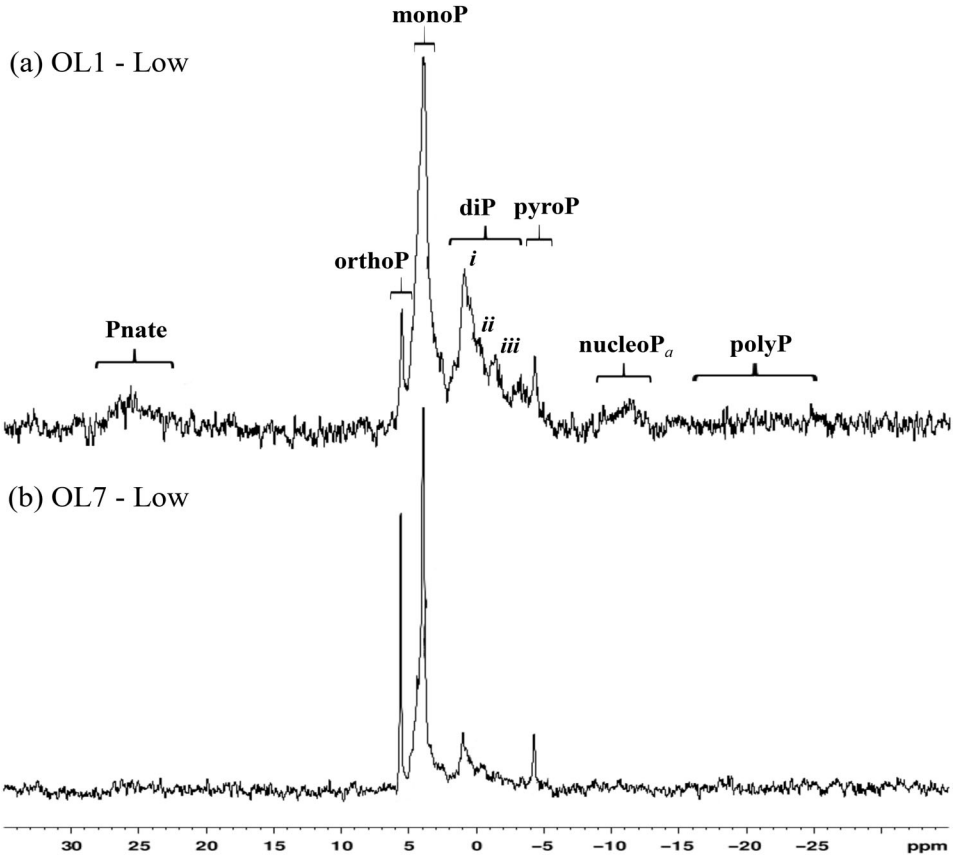

Fig. 2. Two example ^{31}P-NMR spectra of samples taken during low tide in the October 2014 (OL1 – low; **a**) and July 2015 (OL7 – low; **b**). Abbreviated names are referenced as: phosphonates (Pnate), monoesters (monoP), diesters (diP), pyrophosphate (pyroP), ester nucleotide-P (nucleo-P$_\alpha$), and long-chain polyphosphate (polyP). Peaks *i–iii* within the diP component are representative of phospholipids, RNA, and DNA, respectively.

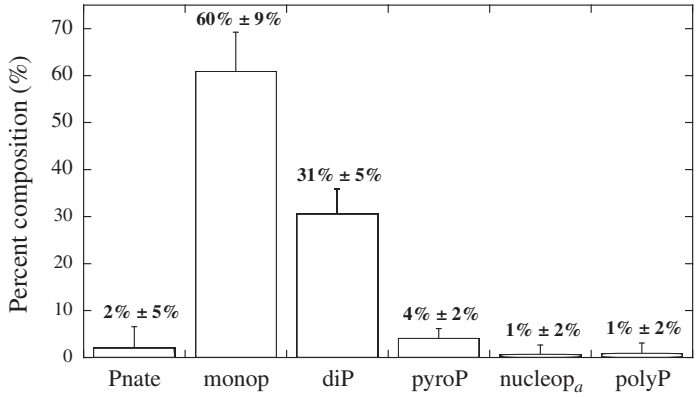

Fig. 3. Mean composition of dissolved organic phosphorus (DOP) over a year-long period (n = 15) from the North Inlet tidal-estuary. Abbreviated names are referenced as: phosphonates (Pnate), monoesters (monoP), diesters (diP), pyrophosphate (pyroP), ester nucleotide-P (nucleo-P_α), and long-chain polyphosphate (polyP). Error bars indicate one standard deviation of the mean.

raw error of these estimates (i.e., instrumentation and post-processing) is approximately ± 5%.

Results

Isolation and solution ^{31}P-NMR preparation

The average ED/RO isolation recovery of DOP was 90% ± 13% and ranged from 73% to 110% (n = 12; Table 1). The first three samples (OL1 – high, low and OL2 – high) used sequential batch processing that produced large uncertainties of recovery estimates (80–160%) and are thus not included in the recovery average. The P mass recovered ranged between 1.0 and 9.5 μmol P with concentrations of lyophilized material ranging between 1.4 and 16.1 μmol P g^{-1}. Single-batch isolates (i.e., OL3–OL8) averaged 2.7 ± 0.7 μmol P g^{-1}. Organic P (OP) comprised on average 88% ± 5% of the isolated P (Iso, Table 1). Despite the extensive processing between isolates, the %OP quantified in ^{31}P-NMR analysis (NMR phase; determined as the percentage of peak area that excludes the orthophosphate peak) was within error of the initial isolate's %OP for 12 of 15 samples (Table 1). Additionally, when the %OP of all four phases (Iso, Lyo, Diss, and NMR) was averaged for each sample, the variation was consistently low (average %RSD of 15 samples was 4% ± 2%). Over the course of the simulated experimental redissolution conditions, DOP was not significantly transformed into SRP (t = 0.691, df = 6, p = 0.516; *see* Supplemental Material).

Molecular composition

Compositional analysis using solution ^{31}P-NMR quantified six classes of DOP: Pnate, monoP, diP, pyroP, nucleoP$_\alpha$, and polyP (Table 2). Example spectra (OL1 – high and OL7 – low) are given in Fig. 2. In all samples, monoP was the greatest contributor to bulk DOP composition (60% ± 9%), double that of diP (31% ± 5%) (Table 2; Fig. 3). PyroP was substantially lower, comprising 4% ± 2% of DOP (Table 2; Fig. 3). Pnate was also a minor component, but highly variable, ranging from below detection to 11% and averaging 2% ± 5% of bulk DOP (Table 2; Fig. 3). NucleoP$_\alpha$ and polyP were often undetectable, representing 1% ± 2% and 1% ± 2% of DOP, respectively (Table 2; Fig. 3).

There were no significant differences in DOP composition between tidal stages, but there was a significant seasonal difference for the Pnate, monoP, and nucleoP classes in the fall compared to other seasons (Table 3). Additionally, the % diP was positively correlated with the % POP (ρ = 0.599, n = 15, p = 0.018; Table S3).

Discussion

Resolving bulk composition

The bulk composition of DOP (i.e., phosphoesters, phosphonates, and phosphonahydrides), as assessed by coupled

Table 3. Averaged components of dissolved organic phosphorus (DOP) composition over seasonal and tidal timescales (shown as percentages). Abbreviated names are referenced as: phosphonates (Pnate), monoesters (monoP), diesters (diP), pyrophosphate (pyroP), ester nucleotide-P (nucleo-P_α), and long-chain polyphosphate (polyP). One standard deviation of the mean is included in parentheses. Significant differences between factor levels (season, tidal stage) are provided from a univariate ANOVA (two-tailed).

	Pnate (%)	monoP (%)	diP (%)	pyroP (%)	nucleoP$_\alpha$ (%)	polyP (%)
Fall (n = 3)	11 (1)	47 (6)	35 (3)	4 (1)	4 (3)	—
Winter (n = 4)	—	65 (4)	28 (8)	5 (2)	—	3 (4)
Spring (n = 4)	—	67 (4)	30 (4)	4 (2)	—	1 (1)
Summer (n = 4)	—	63 (5)	31 (8)	4 (4)	—	—
ANOVA	**	**	N.S.	N.S.	*	N.S.
High (n = 8)	3 (5)	62 (8)	31 (6)	4 (3)	1 (2)	1 (3)
Low (n = 7)	2 (4)	60 (10)	30 (4)	4 (1)	1 (2)	1 (2)
ANOVA	N.S.	N.S.	N.S.	N.S.	N.S.	N.S.

N.S., not significant.
*p < 0.05.
**p < 0.001.

ED/RO and solution ^{31}P-NMR, was similar to past marine DO^{31}P-NMR observations (Kolowith et al. 2001; Sannigrahi et al. 2006; Young and Ingall 2010; Repeta et al. 2016). Phosphoesters dominated DOP composition ranging from 80% to 94% of EDOP (i.e., ED or ED/RO isolated DOP; Young and Ingall, 2010; this study). This is a slightly greater proportion than observed using UDOP (70–75%; UF isolation; Kolowith et al. 2001; Sannigrahi et al. 2006; Repeta et al. 2016). Phosphonates were among the smallest components of EDOP (0–11%) (Young and Ingall, 2010; this study), compared to UDOP (20–25%) (Kolowith et al. 2001; Sannigrahi et al. 2006; Repeta et al. 2016). Phosphoanhydrides, while not detected in open ocean UDOP (Clark et al. 1998; Kolowith et al. 2001), were comparable to other studies assessments using advanced isolation or analytical techniques (ca. 3–13%) (Young and Ingall 2010; Repeta et al. 2016). Still, the primary limitation of bulk classifications of DOP composition has been the inability to refine the specific ecological roles and biomolecular sources of DOP constituents.

From our assessment, five subclasses of P functional groups were identified: monoP and diP (phosphoesters), pyroP and polyP (phosphoanhydrides), and nucleoP$_\alpha$ (phosphoester and phosphoanhydride bonding). The phosphonates pool, however, could not be further resolved. The majority of these subclasses have been previously defined in other marine ^{31}P-NMR (Paytan et al. 2003; Cade-Menun and Paytan 2010), freshwater ^{31}P-NMR (Bai et al. 2015), and enzymatic characterization studies (Monbet et al. 2009; Sato et al. 2013).

Phosphoesters

Phosphoesters are the most dominant P bond class measured in marine seston (Kolowith et al. 2001; Paytan et al. 2003, Sannigrahi et al. 2006) and phytoplankton cultures (Dyhrman et al. 2009; Cade-Menun and Paytan 2010), and mirrors the large phosphoester pool within a typical cell (e.g., nucleic acids, nucleotides, sugars, and lipids) (Geider and LaRoche, 2002). As such, and given the overall dominance of phosphoesters within the DOP pool (~ 90%; Table 2), resolving the bulk class has been of long-standing interest.

The dominant subclass observed was monoP (60% ± 9%; Table 2), although this signal is likely an overestimate due to the following two pieces of evidence. First, despite the consistent proportions of % OP throughout isolation and analysis (Table 1), Bell et al. (2017) found that the alkaline pretreatment for solution ^{31}P NMR degrades ca. 70% of the diP standard compound (RNA) and almost completely degraded a phospholipid standard (L-α-phosphatidylcholine). Similar levels of degradation have been observed in other solution ^{31}P-NMR assessments (Turner et al. 2003; Cade Menun 2015), although Turner et al. (2003) found differential degradation across phospholipid compounds, with L-α-phosphatidyl-L-serine withstanding degradation (88% intact over 24 h), while L-α-phosphatidylcholine was degraded almost immediately (similar to this study). Second, closer inspection of the ^{31}P NMR shifts indicate that monoP is dominated by monophosphate nucleotide peaks (Cade Menun 2015), while phospholipid degradation products (e.g., glycerophosphates) and sugar phosphates (and possibly phytic acid) were identified within the shoulder of the dominant monoP peak (Fig. 2a; Cade Menun 2015).

Therefore, the average diP component measured in this study (31% ± 5%) should be considered closer to a minimum bound. While the bulk diP fraction could be determined, specific diP compounds could not be routinely identified in the ^{31}P NMR spectra (Fig. 2). However, when specific diP peaks were apparent, they corresponded to, in order of decreasing abundance (Fig. 2a [*i–iii*]), intact phospholipids (~ 0.9 ppm; e.g., lipoteichoic acid and various phosphatidyl compounds), RNA (~ 0.0 ppm), and DNA (~ −0.8 ppm) (Cade Menun 2015). Notably, Turner et al. (2003) found RNA to degrade completely after 24 h, while DNA appeared to withstand degradation from alkaline pretreatment conditions, a similar finding of Cade Menun (2015). Karl and Bailiff (1989) also observed RNA to exceed DNA by 3–10 times within the DOP pool, adding support to our hypothesis that much of the monoP signal is due to naturally or analytically degraded RNA. One caveat is that monoP may not be as efficiently recovered using the ED/RO technique relative to diP. While our isolation results indicated almost complete recovery and characterization of the entire DOP pool (Table 1), Bell et al. (2017) found a significant relationship between isolation recovery and MW. Smaller compounds, such as phosphomethyl-glycine (MW = 169), were recovered with 50% efficiency while larger compounds, such as RNA (assumed MW = 3360), were recovered near 80%.

However, we argue that the magnitude of diP degradation for RNA and other diP compounds outweighs the observed difference in size-biased recovery as degradation has a double effect on subclass proportions. Again, we believe our estimates of diP should be considered a minimum bound, although it is very possible that diP may be similar or an even greater proportion of the phosphoester class, relative to monoP, as suggested by several enzymatic characterization studies (Monbet et al. 2009; Sato et al. 2013). Regardless of the proportions between monoP and diP, the dominance of the monophosphate nucleotide signal is not surprising given their critical role as metabolic intermediaries and monomer components of nucleic acids (Kujawinski et al. 2017), which are estimated to comprise a large majority of cellular OP, particularly RNA (Geider and LaRoche 2002).

Phosphoanhydrides

Phosphoanhydrides are comprised of a diverse collection of compounds that exhibit an orthophosphate polymer, which include nucleoside di- and tri-phosphates (e.g., ADP and ATP), polyP, and pyroP, and are integral to a suite of metabolic functions including energy transfer, storage, and metabolic regulation (Kornberg et al. 1999). And while phosphoanhydrides are not necessarily organically bound, they are operationally

defined within the DOP fraction and require enzymatic cleavage to access P (Lin et al. 2016). Phosphoanhydrides, specifically polyP, have also received increased attention due to their recent detection in marine POM, including marine algae (Paytan et al. 2003), sediments (Diaz et al. 2008) and EDOP (Young and Ingall 2010).

In our observations, polyP represented a minor component of DOP, often below the detection limit (1% ± 2%; Fig. 3), while the pyroP class was consistently detected in all samples at a slightly greater proportion (4% ± 2%; Table 2; Fig. 3). Similar to low MW monoP compounds, pyroP may also have been under-recovered. Yet, it is also possible that alkaline dissolution impacted our results by degrading polyP (Bell et al. 2017), although Turner et al. (2003) found their polyP standard to be stable for 9 d in NaOH-EDTA. Terminal P from di- and triphosphate mononucleotides could also be included in the pyroP signal, although this would result in an ester bonded P peak (i.e., nucleoP$_\alpha$) between −9 and −11 ppm (Figs. 2, 3). NucleoP$_\alpha$, however, was only detected in two samples during the fall (OL1 – low and OL2 – high; Table 2). This is not unexpected, as previous estimates have calculated ATP to be less than 2% of the DOP pool (Björkman et al. 2018). While our observed pyroP signal includes contributions from polyP and nucleoP$_\alpha$ classes, several other studies have found pyroP to account for the majority of phosphoanhydrides in marine particulate material (Paytan et al. 2003), cellular cultures (Cade-Menun and Paytan 2010), sediment (Sundareshwar et al. 2001), and freshwater particulate and dissolved P (Bai et al. 2015). Furthermore, work by Blake et al. (2005) has demonstrated the significance of pyrophosphatase and pyroP, the later sourced from triphosate nucleotides, in regulating the $\delta^{18}O$ signature of P_i in seawater. Therefore, the low, but consistent abundance of pyroP observed in our samples encourages a closer examination of pyroP's role in the microbial P cycle and the interplay between phosphoanhydride subclasses.

Phosphonates

Phosphonates, which exhibit direct C—P bonding, exist in cells as functional groups of proteins, lipids, and saccharides (Horsman and Zechel 2017). The phosphonate class has been consistently observed in all ^{31}P-NMR DOP studies, and notably, at a high proportion (~ 20–25% of UDOP) relative to their observed presence in particulate material (Clark et al. 1998; Dyrhman et al. 2009). Young and Ingall (2010) demonstrated that the larger proportion of phosphonates were likely specific to the HMW portion of DOP, yet still, this class was consistently observed at all study sites (7–10% of EDOP) from a broad range of marine environments.

In this study, one of the most notable observations was the low proportion and variable presence of the phosphonate class, which was only observed during the fall season (similar to the nucleoP$_\alpha$ class). In comparison between dissolved and particulate phases, the phosphonate class signal was detected in only 3 of 12 particulate samples we collected and was never more than 3% of the TPP fraction (Table S2). Unfortunately, there was not enough SPM material collected during the fall to achieve a reliable NMR spectrum for comparison with our dissolved samples. In a survey of sinking particulate material from six ecologically distinct regions, Paytan et al. (2003) also found POP composition to vary, exhibiting regional differences, site-specific temporal variation, and the regional presence or absence of measurable phosphonate concentrations. However, we do acknowledge that the seasonal presence of phosphonates, as well as the nucleoP$_\alpha$ class, may have been influenced by the detection limits of the solution ^{31}P-NMR analyses (ca. 0.02 μmol P). Fall samples analyzed roughly four times more material than other seasons and Pnate presence was significantly correlated with the amount of P analyzed (Table 2; Table S3). Given the diversity of compounds across the Pnate spectrum shift range (demonstrated by Repeta et al. 2016), it is possible that our observations were not able to appropriately integrate the complete suite of individual phosphonate compounds present, thus leading to an overall lower detection of the bulk class. Similarly, nucleoP$_\alpha$ may have different spectral shifts depending on the nucleobase and phosphorylation (i.e., ADP vs. ATP) making them harder to identify (Cade Menun 2015). Nonetheless, given the lack of a significant relationship between all other bond classes and sample mass (Table S3), the consistently low proportions of pyroP within all spectra (Table 2), and the resolution of spectra with low isolate P (e.g., OL7 – low; Fig. 1b), our results indicate that phosphonates and nucleoP$_\alpha$ exist at very low proportions (< 4%) and are moderately variable depending on environmental conditions of North Inlet.

Environmental controls of DOP composition

To date, previous DO^{31}P-NMR studies have demonstrated that bulk DOP composition exhibits a high degree of similarity over time and space. However, it is possible that low analytical resolution and limited sampling repetition have obscured variability in DOP composition thus far. Given the considerable evidence of DOC compositional variability (Aluwihare et al. 2002; Osburn et al. 2015), this behavior seems also likely for DOP. Temporal variability in DOP composition is also supported by the seasonality observed in bulk DOP concentrations and DOP components, such as ATP (Björkman and Karl 2005, Lomas et al. 2010), as well as variable seasonal turnover within the DOP pool (Benitez-Nelson and Karl 2002). Such seasonal behavior is generally controlled by the annual timing of SRP supply to a system, and subsequent production and preferential remineralization of organic matter.

From an accompanying study in North Inlet, Bell et al. (2018) observed significant seasonal dynamics for dissolved and particulate P fractions (SRP, DOP, TPP, POP), as well as C:N:P stoichiometry. DOM stoichiometry indicated that fall samples represented conditions of preferential remineralization of P relative to C and N, although maximum

DOM C:N:P ratios occurred in winter (Bell et al. 2018). Bell et al. (2018) also determined material exchange for each tidal cycle and for each dissolved constituent, including the stoichiometry of C, N, and P tidal fluxes. During the fall, DOP was exported from Crab Haul Creek, while SRP, DIN, DOC, and dissolved organic nitrogen (DON) were imported. Net DOP exchange, however, was minimal, with no significant variation in bulk DOP concentrations with tidal stage. Conversely, significant tidal variation was observed for all other dissolved nutrient concentrations measured (DIN, DON, SRP, and DOC). Bell et al. (2018) also tracked changes to the phytoplankton community and found that diatoms dominated community composition throughout the year. This indicates that in North Inlet, autotrophic community composition does not play a dominant role in shaping seasonal biogeochemical behavior, unlike biomass growth and decomposition.

Considering the seasonal biogeochemistry found by Bell et al. (2018) within our study site, as well as previous observations of P seasonal behavior, several hypotheses are proposed to explain compound-specific and bulk DOP observations. Assuming DOP turnover is greater during periods of decreased SRP availability, we hypothesize that late-winter and early-spring months could maintain relatively low concentrations of DOP components, as all compounds would be subjected to an increase in P demand and utilization, and thus be below analytical detection. Bell et al. (2018) found suspended particulate material to be predominantly N-limited throughout the year, although winter–spring months were likely co-limited due to minimized benthic release of P under oxic-sediment conditions (Lillebø et al. 2004). For the phosphonate class, we hypothesize that a relatively higher proportion of phosphonate is produced during the late summer and fall months under conditions of secondary production when phosphonate biosynthesis may be more common among marine bacteria (Horsman and Zechel 2017) vs. eukaryotic phytoplankton (Dyhrman et al. 2009). Despite the preferential remineralization of OM, relatively high P supply allows the phosphonate class to accumulate prior to mixing and export from the tidal creek. This is consistent with Ilikchyan et al. (2009), who found phosphonate hydrolytic-enzyme transcripts to be repressed during periods of increased P supply. With respect to the nucleoP_α subclass, ATP turnover is hypothesized to be rapid and more tightly coupled under lower P_i conditions (Björkman et al. 2018). We argue that nucleoP_α accumulation could have occurred during the fall, when SRP was high, before decreasing in the winter during low OM production and higher P demand. An invariant pyroP signal likely reflects the importance of the ubiquitous intracellular enzyme, pyrophosphatase, which as previously mentioned, appears to be a significant regulating factor in the apparent $\delta^{18}O$ signature and turnover of P_i in seawater (Blake et al. 2005).

As for the two largest subclasses of DOP, monoP and diP showed no statistically significant seasonal trend. However, monoP and diP were inversely correlated throughout the year, with monoP consistently decreasing from winter to fall, while diP increased (Table 3). One might expect that the diP component to increase in relative proportion with organic matter (or biomass), and indeed, a significant positive correlation was observed between the diP subclass and the proportion of organic P in TPP (i.e., %POP; Table S3). However, if a large proportion of diP is RNA, an increase in the monoP signal should also have occurred using our analytical method. The decreased proportion of monoP in the fall may therefore also reflect the high bioavailability of monoP nucleotides that are utilized regardless of P availability. Another driver for the potentially higher proportions of diP is an accumulation of lipid-diP. Phospholipids have been reported to consist of both labile and refractive components (Suzumura and Ingall 2004) and serve a role in DOM preservation (Nagata and Kirchman 1992). This may help explain why the most consistent diP shift corresponds to phospholipid compounds (Fig. 2a-*i*). Although the diP class has been estimated to have longer relative turnover times (Sato et al. 2013), our results suggest that within the entire phosphoester class, there exists a continuum of labilities for each subclass that are likely regulated under seasonal conditions. This may explain the lack of significant seasonal variance between the two phosphoester subclasses, although the analytical challenges brought upon by solution ^{31}P-NMR (i.e., degradation) and ED/RO isolation (i.e., under recovery) further complicates confirming seasonal variances. Moving forward, these results provide a useful and direct comparison with enzymatic studies that focus on relative distributions and in situ utilization of phosphoester subclasses.

DOP behavior across a land–ocean continuum

Nutrient-rich tidal creek systems, such as North Inlet (Fig. 1), allow for significant mixing, turnover, and transformation of coastal ocean and salt-marsh OM (Childers et al. 2002), significantly different from riverine dominated systems that import large amounts of nutrient-depleted terrestrial OM to the coastal zone (Hopkinson et al. 1998. With respect to the DOP pool, our results indicated that tidal mixing imparts no significant compositional differences between high and low tidal stages, likely due to rapid physical turnover and seasonal overprinting (Table 3). Volumetrically, 40% of this study site's tidal creek (Crab Haul Creek; Fig. 1) is exchanged over each tidal cycle, although incomplete mixing maintains effectively longer residence times of biogeochemical constituents (Gardner et al. 2006).

High intensity precipitation events, however, can influence the magnitude of terrestrial material entering salt-marsh estuarine systems. By chance, one sampling event captured such a precipitation event (54 mm over 24 h) during the late-winter (OL4 – low). The ^{31}P-NMR spectra of OL4-low had a unique diP signal with an elevated peak shift that corresponded to

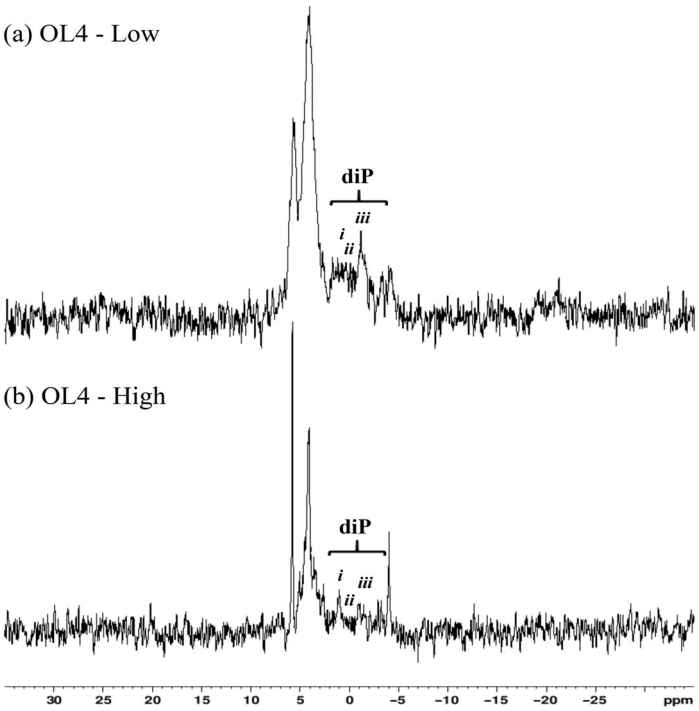

Fig. 4 ^{31}P-NMR spectra for samples taken shortly after a major precipitation event in the late winter (OL4 – Feb 2015). Peaks *i–iii* within the diP (phosphodiester) component are representative of phospholipids, RNA, and DNA, respectively. The sample taken during low tide (**a**) had an elevated peak, relative to all other samples, at roughly −1 ppm, which is indicative of intact DNA. The paired sample taken hours later during high tide (**b**) shows the same peak area now depressed.

DNA, rather than to lipid-diP, which was the predominant diP peak shift in the majority of other samples (Fig. 4a). This observation is supported from wetland soil ^{31}P-NMR studies that observed DNA as the dominant diP component (Turner and Newman 2005). This fraction is assumed to be mostly extracellular DNA, which can be adsorbed onto reactive soil particles and stabilized against nuclease hydrolysis (Pietramellara et al. 2009). The relative decrease in the DNA-diP signal also occurred during high tide, likely due to mixing, but also potentially due to hydrolysis following desorption under saline conditions (Fig. 4b). During the precipitation event, DOP and DON were imported to Crab Haul Creek whereas DOC experienced its greatest individual tidal export (Bell et al. 2018). We suggest that this uncoupling is due to the low nutrient availability that occurred during the late-winter, where organic N and P fractions were quickly utilized, while a surplus of humic-dominated DOC was likely exported. As such, late-winter precipitation events may facilitate a reset of the tidal marsh's annual biogeochemical cycle, importing DOM, which is then desorbed in the tidal creek, and now available to microbial groups that in turn release N and P for utilization by autotrophic communities.

Conclusion: The dynamic equilibrium of DOP

As originally phrased by Waksman and Carey (1935), the DOM pool is in a "state of dynamic equilibrium" (Karl and Björkman 2015). Indeed, DOP tidal exchange was observed to be near a net balance and consistently decoupled from DOC and DON behavior at our study site (Bell et al. 2018). Our results demonstrated that estuarine DOP was dominated by monomer and polymer components of nucleic acids. Given their essential role in metabolism and cell operation, and the demonstrated environmental potential for enzymatic hydrolysis, the composition of DOP represents an even tighter dynamic equilibrium with its source material, than either DOC or DON, rapidly turning over under periods of low P supply. However, under reduced P demand, decoupling may occur, allowing less reactive components to accumulate and be subjected to increased physical controls. The consistent proportion of phosphonates in HMW DOP observed in other marine studies may reflect accumulation under such conditions. Furthermore, the slightly greater proportion of phosphonates in oceanic DOP, relative to observations in this study, may also indicate more localized production.

Overall, the increased resolution of DOP composition, coupled with the well-resolved biogeochemical context of the tidal estuary, revealed new insights and highlight the potential for a better understanding of marine P cycling across regimes. For example, the hypothesized seasonal shifts in DOP composition enable further evaluation of the potential changes in microbial source contribution (auto- and heterotrophic), while increased resolution allows specific biomolecular class bioavailability to be (re)evaluated at the community and species level. Comparisons at the bulk-level showed that estuarine DOP composition exhibit similar abundances of phosphoesters, phosphonates, and phosphoanhydrides, consistent with previous work from the coastal and open ocean (Kolowith et al. 2001; Sannigrahi et al. 2006; Young and Ingall 2010). This degree of similarity indicates that the fundamental interactions (i.e., compound-specific production and utilization) that drive the microbial P cycle are conserved across all marine environments, although the fate of DOP (i.e., utilization or export) and the degree of seasonal variability for each DOP subclass, rely on local conditions of P demand.

References

Aluwihare, L. I., D. J. Repeta, and R. F. Chen. 2002. Chemical composition and cycling of dissolved organic matter in the mid-Atlantic Bight. Deep-Sea Res. II Top. Stud. Oceanogr. **49**: 4421–4437. doi:10.1016/S0967-0645(02)00124-8

Arrigo, K. R. 2005. Marine microorganisms and global nutrient cycles. Nature **437**: 349.

Aspila, K. I., H. Agemian, and A. S. Y. Chau. 1976. A semi-automated method for the determination of inorganic,

organic and total phosphate in sediments. Analyst **101**: 187–197. doi:10.1039/AN9760100187

Bai, X. L., Y. K. Zhou, J. H. Sun, J. H. Ma, H. Y. Zhao, and X. F. Liu. 2015. Classes of dissolved and particulate phosphorus compounds and their spatial distributions in the water of a eutrophic lake: A 31P NMR study. Biogeochemistry **126**: 227–240. doi:10.1007/s10533-015-0155-7

Bell, D. W., P. Pellechia, L. R. Chambers, A. F. Longo, K. M. McCabe, E. D. Ingall, and C. R. Benitez-Nelson. 2017. Isolation and molecular characterization of dissolved organic phosphorus using electrodialysis-reverse osmosis and solution 31P-NMR. Limnol. Oceanogr.: Methods. **15**: 436–452. doi:10.1002/lom3.10171

Bell, D. W., S. Denham, E. M. Smith, and C. R. Benitez-Nelson. 2018. Temporal variability in ecological stoichiometry and material exchange in a tidally dominated estuary (North Inlet, South Carolina) and the impact on community nutrient status. Estuaries Coasts **41**: 2223–2239. doi:10.1007/s12237-018-0430-7

Benitez-Nelson, C. R., and D. M. Karl. 2002. Phosphorus cycling in the North Pacific Subtropical Gyre using cosmogenic 32P and 33P. Limnol. Oceanogr. **47**: 762–770. doi:10.4319/lo.2002.47.3.0762

Björkman, K. M., and D. M. Karl. 2005. Presence of dissolved nucleotides in the North Pacific Subtropical Gyre and their role in cycling of dissolved organic phosphorus. Aquat. Microb. Ecol. **39**: 193–203. doi:10.3354/ame039193

Björkman, K. M., S. Duhamel, S., M.J. Church, and D.M. Karl. 2018. Spatial and temporal dynamics of inorganic phosphate and adenosine-5′-triphosphate in the North Pacific Ocean. Front. Mar. Sci. **5**: 1–14. doi:10.3389/fmars.2018.00235

Blake, R. E., J. R. O'Neil, and A. V. Surkov. 2005. Biogeochemical cycling of phosphorus: Insights from oxygen isotope effects of phosphoenzymes. Am. J. Sci. **305**: 596–620. doi:10.2475/ajs.305.6-8.596

Cade-Menun, B. J. 2005. Characterizing phosphorus in environmental and agricultural samples by 31 P nuclear magnetic resonance spectroscopy. Talanta **66**: 359–371. doi:10.1016/j.talanta.2004.12.024

Cade-Menun, B. J. 2015. Improved peak identification in 31 P-NMR spectra of environmental samples with a standardized method and peak library. Geoderma **257**: 102–114. doi:10.1016/j.geoderma.2014.12.016

Cade-Menun, B. J., and A. Paytan. 2010. Nutrient temperature and light stress alter phosphorus and carbon forms in culture-grown algae. Mar. Chem. **121**: 27–36. doi:10.1016/j.marchem.2010.03.002

Cembella, A. D., N. J. Antia, and P. J. Harrison. 1982. The utilization of inorganic and organic phosphorous compounds as nutrients by eukaryotic microalgae: A multidisciplinary perspective: Part I. Crit. Rev. Microbiol. **10**: 317–391. doi:10.3109/10408418209113567

Chambers, L. R., and others. 2016. Enhanced dissolved organic matter recovery from saltwater samples with coupled electrodialysis and solid phase extraction. Aquat. Geochem **22**: 555–572. doi:10.1007/s10498-016-9306-2

Childers, D. L., J. W. Day, and H. N. McKellar. 2002. Twenty more years of marsh and estuarine flux studies: Revisiting Nixon (1980), p. 391–423. *In* M. P. Weinstein and D. A. Kreeger [eds.], Concepts and controversies in tidal marsh ecology. Springer.

Clark, L. L., E. D. Ingall, and R. Benner. 1998. Marine phosphorus is selectively remineralized. Nature **393**: 426–426.

Diaz, J., E. Ingall, C. Benitez-Nelson, D. Paterson, M. D. de Jonge, I. McNulty, and J. A. Brandes. 2008. Marine polyphosphate: A key player in geologic phosphorus sequestration. Science **320**: 652–655. doi:10.1126/science.1151751

Dyhrman, S. T., C. R. Benitez-Nelson, E. D. Orchard, S. T. Haley, and P. J. Pellechia. 2009. A microbial source of phosphonates in oligotrophic marine systems. Nat. Geosci. **2**: 696–699.

Gardner, L. R., B. Kjerfve, and D. M. Petrecca. 2006. Tidal fluxes of dissolved oxygen at the North Inlet - Winyah Bay national estuarine research reserve. Estuar. Coast. Shelf Sci. **67**: 450–460. doi:10.1016/j.ecss.2005.12.002

Geider, R., and J. La Roche. 2002. Redfield revisited: Variability of C:N:P in marine microalgae and its biochemical basis. Eur. J. Phycol. **37**: 1–17. doi:10.1017/S0967026201003456

Green, N. W., E. M. Perdue, G. R. Aiken, K. D. Butler, H. Chen, T. Dittmar, J. Niggemann, and A. Stubbins. 2014. An intercomparison of three methods for the large-scale isolation of oceanic dissolved organic matter. Mar. Chem. **161**: 14–19. doi:10.1016/j.marchem.2014.01.012

Hopkinson, C. S., Jr., and others. 1998. Terrestrial inputs of organic matter to coastal ecosystems: An intercomparison of chemical characteristics and bioavailability. Biogeochemistry. **43**: 211–234.

Hopkinson, C. S., Jr., J. J. Vallino, and A. Nolin. 2002. Decomposition of dissolved organic matter from the continental margin. Deep-Sea Res. II Top. Stud. Oceanogr. **49**: 4461–4478. doi:10.1016/S0967-0645(02)00125-X

Horsman, G. P., and D. L. Zechel. 2017. Phosphonate biochemistry. Chem. Rev. **117**: 5704–5783. doi:10.1021/acs.chemrev.6b00536

Howarth, R., F. Chan, D. J. Conley, J. Garnier, S. C. Doney, R. Marino, and G. Billen. 2011. Coupled biogeochemical cycles: Eutrophication and hypoxia in temperate estuaries and coastal marine ecosystems. Front. Ecol. Enviro. **9**: 18–26. doi:10.1890/100008

Ilikchyan, I. N., R. M. L. McKay, J. P. Zehr, S. T. Dyhrman, and G. S. Bullerjahn. 2009. Detection and expression of the phosphonate transporter gene phnD in marine and freshwater picocyanobacteria. Environ. Microbiol. **11**: 1314–1324. doi:10.1111/j.1462-2920.2009.01869.x

Karl, D. M. 2014. Microbially mediated transformations of phosphorus in the sea: New views of an old cycle. Ann.

Rev. Mar. Sci. **6**: 279–337. doi:10.1146/annurev-marine-010213-135046

Karl, D. M., and D. M. Bailiff. 1989. The measurement and distribution of dissolved nucleic acids in aquatic environments. Limnol. Oceanogr. **34**: 543–558. doi:10.4319/lo.1989.34.3.0543

Karl, D. M., and K. M. Björkman. 2015. Dynamics of DOP, p. 233–334. *In* D. A. Hansell and C. A. Carlson [eds.], Biogeochemistry of marine dissolved organic matter. Academic Press.

Kolowith, L. C., E. D. Ingall, and R. Benner. 2001. Composition and cycling of marine organic phosphorus. Limnol. Oceanogr. **46**: 309–320. doi:10.4319/lo.2001.46.2.0309

Koroleff, F. 1983. Simultaneous oxidation of nitrogen and phosphorus compounds by persulfate, p. 205–206. *In* K. Grasshoff, M. Ehrhardt, and K. Kremling [eds.], Methods of seawater analysis, 2nd ed. Verlag Chemie.

Kornberg, A., N. N. Rao, and D. Ault-Riche. 1999. Inorganic polyphosphate: A molecule of many functions. Annu. Rev. Biochem. **68**: 89–125. doi:10.1146/annurev.biochem.68.1.89

Kujawinski, E. B., K. Longnecker, H. Alexander, S. T. Dyhrman, C. L. Fiore, S. T. Haley, and W. M. Johnson. 2017. Phosphorus availability regulates intracellular nucleotides in marine eukaryotic phytoplankton. Limnol. Oceanogr.: Lett. **2**: 119–129. doi:10.1002/lol2.10043

Letscher, R. T., and J. K. Moore. 2015. Preferential remineralization of dissolved organic phosphorus and non-Redfield DOM dynamics in the global ocean: Impacts on marine productivity, nitrogen fixation, and carbon export. Global Biogeochem. Cycles **29**: 325–340. doi:10.1002/2014GB004904

Lillebø, A. I., J. M. Neto, M. R. Flindt, J. C. Marques, and M. A. Pardal. 2004. Phosphorous dynamics in a temperate intertidal estuary. Estuar. Coast. Shelf Sci. **61**: 101–109. doi:10.1016/j.ecss.2004.04.007

Lin, S., R. W. Litaker, and W. G. Sunda. 2016. Phosphorus physiological ecology and molecular mechanisms in marine phytoplankton. J. Phycol. **52**: 10–36. doi:10.1111/jpy.12365

Lomas, M. W., A. L. Burke, D. A. Lomas, D. W. Bell, C. Shen, S. T. Dyhrman, and J. W. Ammerman. 2010. Sargasso Sea phosphorus biogeochemistry: An important role for dissolved organic phosphorus (DOP). Biogeosciences **7**: 695–710. doi:10.5194/bg-7-695-2010

Lønborg, C., and X. A. Álvarez-Salgado. 2012. Recycling versus export of bioavailable dissolved organic matter in the coastal ocean and efficiency of the continental shelf pump. Global Biogeochem. Cycles **26**: 1–12. doi:10.1029/2012GB004353

Luo, H., R. Benner, R. A. Long, and J. Hu. 2009. Subcellular localization of marine bacterial alkaline phosphatases. Proc. Natl. Acad. Sci. USA **106**: 21219–21223. doi:10.1073/pnas.0907586106

Martinez, A., G. W. Tyson, and E. F. DeLong. 2010. Widespread known and novel phosphonate utilization pathways in marine bacteria revealed by functional screening and metagenomic analyses. Environ. Microbiol. **12**: 222–238. doi:10.1111/j.1462-2920.2009.02062.x

Monaghan, E. J., and K. C. Ruttenberg. 1999. Dissolved organic phosphorus in the coastal ocean: Reassessment of available methods and seasonal phosphorus profiles from the Eel River shelf. Limnol. Oceanogr. **44**: 1702–1714. doi:10.4319/lo.1999.44.7.1702

Monbet, P., I. D. McKelvie, and P. J. Worsfold. 2009. Dissolved organic phosphorus speciation in the waters of the Tamar estuary (SW England). Geochim. Cosmochim. Acta **73**: 1027–1038. doi:10.1016/j.gca.2008.11.024

Moore, C. M., and others. 2013. Processes and patterns of oceanic nutrient limitation. Nat. Geosci. **6**: 701–710.

Nagata, T., and D. L. Kirchman. 1992. Release of macromolecular organic complexes by heterotrophic marine flagellates. Mar. Ecol. Prog. Ser. **83**: 233–240.

Osburn, C. L., M. P. Mikan, J. R. Etheridge, M. R. Burchell, and F. Birgand. 2015. Seasonal variation in the quality of dissolved and particulate organic matter exchanged between a salt marsh and its adjacent estuary. Eur. J. Vasc. Endovasc. Surg. **120**: 1430–1449. doi:10.1002/2014JG002897

Paytan, A., B. J. Cade-Menun, K. McLaughlin, and K. L. Faul. 2003. Selective phosphorus regeneration of sinking marine particles: Evidence from 31 P-NMR. Mar. Chem. **82**: 55–70. doi:10.1016/S0304-4203(03)00052-5

Pietramellara, G., J. Ascher, F. Borgogni, M. T. Ceccherini, G. Guerri, and P. Nannipieri. 2009. Extracellular DNA in soil and sediment: Fate and ecological relevance. Biol. Fertil. Soils **45**: 219–235.

Repeta, D. J., S. Ferrón, O. A. Sosa, C. G. Johnson, L. D. Repeta, M. Acker, and D. M. Karl. 2016. Marine methane paradox explained by bacterial degradation of dissolved organic matter. Nat. Geosci. **9**: 884–887. doi:10.1038/ngeo2837Ruttenberg

Ruttenberg, K. C., and S. T. Dyhrman. 2005. Temporal and spatial variability of dissolved organic and inorganic phosphorus, and metrics of phosphorus bioavailability in an upwelling-dominated coastal system. J. Geophys. Res.: Oceans **110**: C10. doi:10.1029/2004JC002837

Sannigrahi, P., E. D. Ingall, and R. Benner. 2006. Nature and dynamics of phosphorus-containing components of marine dissolved and particulate organic matter. Geochim. Cosmochim. Acta **70**: 5868–5882. doi:10.1016/j.gca.2006.08.037

Sato, M., F. Sakuraba, and F. Hashihama. 2013. Phosphate monoesterase and diesterase activities in the North and South Pacific Ocean. Biogeosciences **10**: 7677–7688. doi:10.5194/bg-10-7677-2013

Simpson, A. J., M. J. Simpson, and R. Soong. 2012. Nuclear magnetic resonance spectroscopy and its key role in environmental research. J. Chem. Ecol. **46**: 11488–11496. doi:10.1021/es302154w

Sundareshwar, P. V., J. T. Morris, P. J. Pellechia, H. J. Cohen, D. E. Porter, and B. C. Jones. 2001. Occurrence and ecological implications of pyrophosphate in estuaries. Limnol. Oceanogr. **46**: 1570–1577. doi:10.4319/lo.2001.46.6.1570

Suzumura, M., and E. D. Ingall. 2004. Distribution and dynamics of various forms of phosphorus in seawater: Insights from field observations in the Pacific Ocean and a laboratory experiment. Deep-Sea Res. I Oceanogr. Res. Pap. **51**: 1113–1130. doi:10.1016/j.dsr.2004.05.001

Turner, B. L., N. Mahieu, and L. M. Condron. 2003. The phosphorus composition of temperate pasture soils determined by NaOH–EDTA extraction and solution 31P NMR spectroscopy. Org. Geochem. **34**: 1199–1210. doi:10.1016/S0146-6380(03)00061-5

Turner, B. L., and S. Newman. 2005. Phosphorus cycling in wetland soils. J. Environ. Qual. **34**: 1921–1929. doi:10.2134/jeq2005.0060

Van Mooy, B. A., and others. 2009. Phytoplankton in the ocean use non-phosphorus lipids in response to phosphorus scarcity. Nature. **458**: 69–72.

Waksman, S. A., and C. L. Carey. 1935. Decomposition of organic matter in sea water by bacteria: II. Influence of addition of organic substances upon bacterial activities. J. Bacteriol. **29**: 545–561.

Yamaguchi, H., M. Yamaguchi, K. Fukami, M. Adachi, and T. Nishijima. 2005. Utilization of phosphate diester by the marine diatom *Chaetoceros ceratosporus*. J. Plankton Res. **27**: 603–606. doi:10.1093/plankt/fbi027

Young, C. L., and E. D. Ingall. 2010. Marine dissolved organic phosphorus composition: Insights from samples recovered using combined electrodialysis/reverse osmosis. Aquat. Geochem. **16**: 563–574. doi:10.1007/s10498-009-9087-y

Acknowledgments

This work was supported by the National Science Foundation (OCE-1061094 to CBN) the SPARC Graduate Research Grant program (Office of the Vice President for Research, University of South Carolina to DWB), the Kathryn D. Sullivan Earth and Marine Science Fellowship (S.C. Space Grant and Sea Grant Consortiums to DWB), and the Slocum-Lunz Foundation (to DWB). We also give special thanks to Kelly McCabe for her efforts in sample processing, as well as Luke Chambers and Amelia Longo for their critical role in developing the ED/RO instrumentation and methodology.

Conflict of interest

The authors declared no potential conflicts of interest.

Submitted 31 October 2019
Revised 21 March 2020
Accepted 21 May 2020

Associate editor: Benjamin Van Mooy